A 3-DOF Actuated Robot Based on a Minimal Tensegrity Configuration

Josep M. Mirats-Tur and Josep Camps

Abstract—This paper presents a realization of a tensegrity based robot composed of a 3-bar symmetric prism-like minimal tensegrity configuration. Statics and kinematics are studied presenting the workspace for the designed robot. After a detailed implementation description of the physical robot, some trajectories within its workspace are analyzed. While our long term objective is provide to the community mobile tensegrity based robots, this work studies a case in which the robot is anchored to the ground. This provides us a first insight of how these structures should be actuated and sensed in order to produce movement.

Index Terms—Tensegrity structures, mechanism design.

I. INTRODUCTION

FROM an engineering point of view tensegrity are a special class of structures whose elements may simultaneously perform the purposes of structural force, actuation, sense, and feedback control. They have a very high resistance/weight coefficient and are easily deformable. In such kind of structures, theoretically, pulleys or other kind of actuators may stretch/shorten some of the constituting elements in order to substantially change their form with a little variation of the structure's energy. [7, 8] demonstrated that tensegrity structures are very similar to cytoskeleton structures of unicellular organisms, some of which are known to move. They are also very similar to muscle-skeleton structures of high efficiency land animals that can reach speeds up to 60 mph. As reported by [24] these beings incorporate tensional elements in their muscle-skeleton system such that they maintain the structure integrity while acting it, storing and distributing energy [11].

Due to these similarities with such organisms we think that tensegrity structures may be a good candidate to construct mobile robots with arbitrary forms and capable of self-deformation in order to adapt efficiently to the environment where they work. Up to now tensegrity have been mainly used for static applications where the length of all members is kept constant and actuation is performed only to compensate for external perturbations. In the last decades the tensegrity framework has been also used to build deployable structures although the tensegrity paradigm has not been fully exploited either. It is not since very recent years that we find some relevant works towards this goal: for instance, [1] put together several simple tensegrity structures to build a redundant manipulator robot. [17] and [13] proposed different self-propelled tensegrity architectures to build mobile robots.

Josep M. Mirats Tur (jmirats@cetaqua.com), Cetaqua - Centro Tecnológico del Agua, Passeig dels Til.lers 3, 08034, Barcelona, Spain

Josep Camps is currently at the Institut de Robòtica i Informàtica Industrial, C/Llorens i Artigas, 4-6. 08028, Barcelona, Spain.

The purpose of this paper is to demonstrate the feasibility of constructing robots using tensegrity structures. Mobile robotics is our long term objective but first, in order to understand how these structures can be actuated and sensed, we face up the problem of manipulators, i.e. with fixed base. So we present in this paper the implementation, including design and construction details, of a robot based on a 3 bar prism-like tensegrity in a 3D minimal configuration. The designed mechanism is capable of following any desired trajectory inside its workspace.

This paper is organized as follows. An introductory geometric robot description is given in section II. Static and kinematic analysis is performed in section III where results such as the workspace of the constructed robot are provided. Next, section IV hands in a detailed description of the implementation of the presented robot: simulation results, mechanics and electronics implementation. Some real results comprising different trajectories followed by this tensegrity based robot are reported in section V. Finally, main conclusions of this work are outlined in section VI.

II. ROBOT DESCRIPTION

This work deals with the design, construction and validation stages of a new kind of deformable robot based on an actuated tensegrity structure, the octahedral tensegrity system first introduced by [20] and [3]. A schematic of the designed robot is given in figure 1 representing a minimal tensegrity configuration in stable equilibrium. *Minimal* means, in this context, that the number of cables used to link the rigid elements are the minimum required to give stability (in terms of rigidity) to the structure in the $3D$ space. This number is 9 in the case of the octahedral tensegrity; note, however, that we fixed the lower nodes of the structure so the 3 lower cables disappear as depicted in figure 1.

A fixed reference frame is considered to be located at node n_1 being the y axis oriented towards node n_2, as depicted in the figure. The three lower nodes labeled as n_1, n_2, n_3, have been fixed to the ground so eliminating possible rigid displacements of the whole structure in the space. Therefore, being a the side of the lower base triangle, the vectors of position for these nodes with respect to the chosen reference frame can be stated as:

$$\mathbf{p}_1 = (0,0,0)^T$$
$$\mathbf{p}_2 = (0,a,0)^T \quad\quad (1)$$
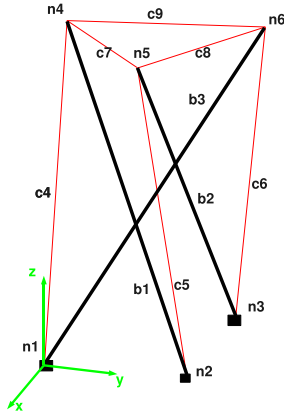$$\mathbf{p}_3 = (-sin(60*pi/180)*a, cos(60*pi/180)*a, 0)^T$$

Fig. 1. Minimal tensegrity in stable configuration representing the designed robot. Cables are thin red lines while bars are the thick black ones.

Edges between the three lower nodes have been eliminated since they have no function at all. Upper nodes are linked to the lower ones by three actuated bars which may vary their lengths; in fact, this can be mathematically seen as a strut with an upper elongation limit. Bar b_1 links nodes n_2 and n_4, bar b_2 nodes n_3 and n_5, and bar b_3 links node n_1 to node n_6. Please note that the ordering of bars and nodes may be arbitrarily chosen provided the right connections between them. Position of the upper nodes can hence be expressed as:

$$\mathbf{p}_4 = \mathbf{p}_2 + l_{b_1}\mathbf{b}_1$$
$$\mathbf{p}_5 = \mathbf{p}_3 + l_{b_2}\mathbf{b}_2 \qquad (2)$$
$$\mathbf{p}_6 = \mathbf{p}_1 + l_{b_3}\mathbf{b}_3$$

where l_{b_i} denotes the current longitude of bar b_i and $\mathbf{b}_i$ a unit vector on the direction of the $i-th$ bar. This could alternatively be expressed using two rotation angles for each bar, pitch and yaw, which respectively represent the angle of the bar with respect to the xy plane, β_i, and the angle of the bar projection onto the xy plane with respect the x axis, α_i.

$$\mathbf{b}_i = \begin{pmatrix} cos\alpha_i cos\beta_i \\ sin\alpha_i cos\beta_i \\ sin\beta_i \end{pmatrix} \qquad (3)$$

In order to complete the tensegrity structure tensile elements are needed. As the bars are actuated each time some or all of the bars lengths change the longitude of whichever tensile element used has to be changed as well. This fact ensures the structure is maintained in a stable position. We have chosen to use springs instead of cables so as to assure the tensile elements of the structure passively adapt to the required length when changing the bar lengths. Also, we assure that the structure always stays in a minimum energy configuration once the actuators are locked. Hence, six springs are needed c_4 to c_9 which respectively link nodes n_1 to n_4, n_2 to n_5, n_3 to n_6, for the vertical springs, and n_4 to n_5, n_5 to n_6 and n_6 to n_4 for the horizontal springs on the upper triangular platform. These springs are considered to be massless and linear elastic with stiffness constant k equal for all of them and rest-length

l_{c_0}. The stiffness of the bars is assumed to be infinite with respect to that of the springs.

The reference configuration for our robot is the first corresponding to a proper tensegrity configuration, the one from which the springs are always in tension. A proper configuration can be found by using a form-finding technique. It is beyond the scope of this paper to talk about such techniques, please refer for instance to [23] for more details. So our first proper tensegrity configuration corresponds to, using $a = 57cm$ and $l_{c_0} = 38cm$, an elongation of the bars of $67cm$. However, control inputs can be generated from $l_b \in [55, 92]cm$. Note that for the range $l_b \in [55, 67)cm$ the robot is not a valid tensegrity since the springs are not in tension. This range of control inputs should not be considered here. Nevertheless it is worth to mention since the designed robot can be deployed from a total folded configuration to a 3D simplex tensegrity structure by means of the considered actuators.

We note that the designed robot has a total of 9 degrees of freedom, since each node could move in the three axes but we have 9 constraints imposed by the three lower nodes, which are fixed. However, only three of them are actuated. As a matter of fact, the three controllable dofs, that is our output vector, are the $\boldsymbol{\lambda} = (x, y, z)$ coordinates of the centre of mass of the upper triangle driven by the control inputs $\mathbf{u} = (l_{b_1}, l_{b_2}, l_{b_3})$. The remaining dofs are constrained by the potential energy of the springs, it must reach a minimum so as to drive the structure to a stable position. Given a fixed length for each of the bars together with a set of nodal forces there is a unique possible stable position of the robot corresponding to a self-stress configuration, that is a configuration where the null space of the robot's equilibrium matrix ([18]) is not empty. Note that as the robot is sub-actuated and we used springs instead of cables, and although the actuators are locked, it will move to a different equilibrium configuration when external forces are exerted onto the structure nodes.

III. STATIC AND KINEMATIC ANALYSIS

We devote our attention to the statics and kinematics. In a tensegrity structure with actuators capable of changing the length of some of its elements, the relations between input (in our case the length of the bars) and output variables (the centre of mass of the upper platform) will, in general, depend on internal forces (tension in the springs) as well as external ones. The dynamic model of the system under study is left for future works, by now the interested reader could check our ongoing work in this field in [14] or [4].

The study of the static and dynamic characteristics of such structures has previously received some attention by the scientific community in other areas. Some analytic solutions to the static problem were given by [16], [10], or more recently, a quite complete static analysis review was given by [5]. The dynamics of tensegrity were first studied by [15]. [9] studied dynamic particle models while considering the bars to be massless; other studies, [19] or [21] consider mass on bars. Also non-linear models and their linearisation have been considered by [22]. All those studies consider statics and dynamics from a structural point of view, for example the

behaviour of a tensegrity dome under heavy winds, but have not considered the possibility of a tensegriy with self-motion capability.

We would be interested in solving both, the direct and the inverse kinematic problems. The first is related to the calculation of $\boldsymbol{\lambda}$ when the external forces on the upper nodes $\mathbf{f}_{ext}^T = (\mathbf{f}_4^T, \mathbf{f}_5^T, \mathbf{f}_6^T)$ and the control inputs $\mathbf{u}$ are given. On the other hand, the second problem is related to find $\mathbf{u}$ for a desired $\boldsymbol{\lambda}$ when a force is exerted onto the nodes of the upper platform.

In order to solve these problems we can take a look at the equilibrium equations of the structure. For a tensegrity structure to be in an equilibrium configuration

$$\mathbf{R}(\mathbf{p})^T \boldsymbol{\gamma} = \mathbf{f}_{ext} \qquad (4)$$

where $\mathbf{R}(\mathbf{p})^T$ denotes the equilibrium matrix of the structure relating the internal forces in the elements $\boldsymbol{\gamma}$ to the nodal forces $\mathbf{f}_{ext}$. The vector $\mathbf{p}$ contains the coordinates of the nodes; is a concatenation of the $\mathbf{p}_i$ vectors. In general, for a structure with e elements and n nodes, $\mathbf{R}(\mathbf{p})^T$ has dimension $nd \times e$ being d the dimension of the realization space. This matrix has a column for each element and a row for each node and dimension which is full of $0's$ except for the elements in the rows corresponding to the element terminal nodes.

A 3-bar prism-like tensegrity has an equilibrium matrix of dimension $18x12$ meaning 18 highly non-linear equations for 15 unknowns. In our case, as we fixed the lower nodes to the ground, the equilibrium matrix has dimension $9x9$ so we have a system of 9 non-linear equations for 9 unknowns. Those are the coordinates of the upper nodes from which we can compute the internal force provided the rest lengths of the springs, their stiffness constants and assuming a linear spring model. Hence, in general we can not find a close solution to those equations.

We rather looked at these problems from energetic considerations. As was demonstrated by [2], for a tensegrity structure to be at an equilibrium configuration it should be at a minimum of its potential energy. The potential energy considering the gravitational force is given by the expression:

$$U = \frac{1}{2}k \sum_{j=1}^{n_c} (l_{c_j} - l_{c_{j0}})^2 + \sum_{j=1}^{n_b} mgh_j$$

where l_c, l_b are, respectively, the lengths for cables and bars, m is the mass of the bars, considered equal for all of them, g is the gravitational constant, and $h_j = \frac{1}{2}l_{b_j} sin\beta_j$ is the height of the bar's centre of mass. Note the dependency of the l_c on the i, j nodes coordinates $l_c^2 = (\mathbf{p}_j - \mathbf{p}_i)^T(\mathbf{p}_j - \mathbf{p}_i)$.

At a first glance one may think in getting proper equations by taking derivatives of the potential energy with respect the considered generalized coordinates (whether the unitary vectors of the bars or the angles α_i, β_i); but this is in general not enough since we have to observe some constraints in order to be at a tensegrity configuration. These constraints are mainly given by maintaining the springs in tension and complying equations 4.

So we face a problem of non-linear minimization with non-linear constraints which can be solved by non-linear programming using, for instance, a penalty method. This has been the approach followed in this work. Details on the optimization technique used can be found in [6].

Now, for the direct kinematic problem we provide $\mathbf{u}$ as well as the external forces and solve an optimization problem. In this way if we discretize the actuator space the workspace of our robot can be computed. Figures 2 and 3 show the possible positions for the upper nodes as well as the workspace for the proposed robot considering the output as the centre of mass of the upper platform. Bars have allowed to change length between $l_b = 67cm$ and $l_b = 92cm$ with $5mm$ increments.
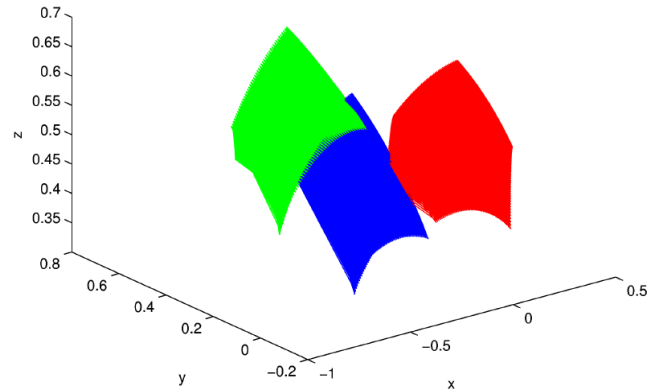

Fig. 2. Admissible positions for the upper nodes of the robot when the bar lengths are allowed to change in the interval $l_b \in [67, 92]cm$. Blue is for node n_4, red n_5 and green n_6.
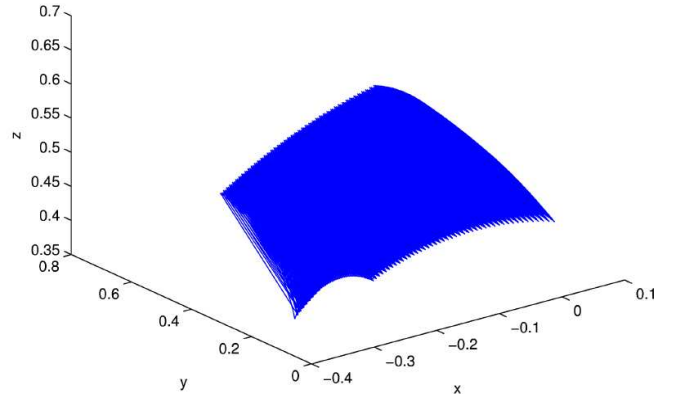

Fig. 3. Workspace for the proposed robot considering the output as the centre of mass of the upper platform when the bar lengths are allowed to change in the interval $l_b \in [67, 92]cm$.

The inverse kinematic problem can be solved as well by solving an optimization algorithm. Given a final desired configuration we first compute the closer equilibrium configuration to it by solving a form-finding procedure. Then, values for the required length of the bars and hence the required control inputs are obtained.

IV. IMPLEMENTATION

The implemented robot is basically composed of three actuated bars and nine passive strings in the form of springs. It was necessary to design an electronic motion control unit for the actuators as well as a force sensor acquisition system. We analyse in this section three basic items of the robot implementation: previous simulation, design of the mechanic parts and control hardware.

A. Simulation

As a previous step to the physical implementation of the robot it was necessary to simulate the full structure with the aim of estimating its key parameters: length of the bars, the motor torque required to perform a given bar elongation and the springs stiffness constant and rest lengths.

Simulation starting point is a stable configuration for the 3-bar tensegrity structure. In this case the six nodes coordinates were obtained by solving a form finding process [6] considering a bar length of $55cm$. Once the coordinates of the nodes were obtained a model was built using Adams, a physical simulation program of mechanical assemblies. A screen-shot of the complete robot is shown in figure 4.

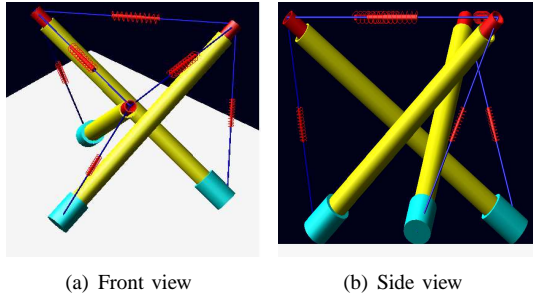

(a) Front view   (b) Side view

Fig. 4.   Preview of the prototype structure using a simulation software.

The form finding process did not take into account the gravity field, so at the beginning the structure is not in a well-balanced configuration. The first performed simulation was letting the structure to freely oscillate until it achieved the equilibrium state. This is shown in Figure 5 where the force exerted on the three springs entering a node during the transitory mode are also shown. The final equilibrium state gives us enough information to know two of the key parameters: the minimum initial length of the springs (all of them considered to be equal) and the minimum constant force that they should support.

For the bars we want to control their lengths using DC motors. In order to estimate the necessary force to displace the nodes and, hence, determine the proper torque of the motors, a different simulation is required; see figure 6.

B. Robot Mechanics

The main mechanical issue is the design of the actuated bars. They have been made up of aluminium due to its low weight. Bar length change is based on the screw mechanism: a screw thread is fixed to the motor axis and the corresponding
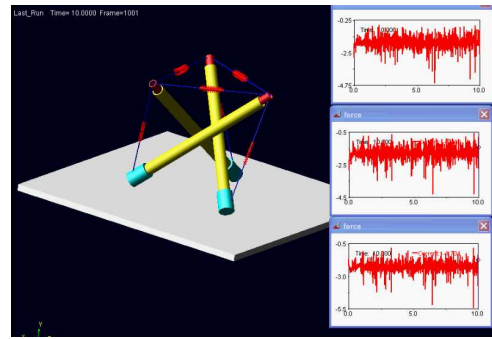

Fig. 5.   Transient simulation before arriving to equilibrium configuration. On the right, real force exerted on the three springs linking each node.
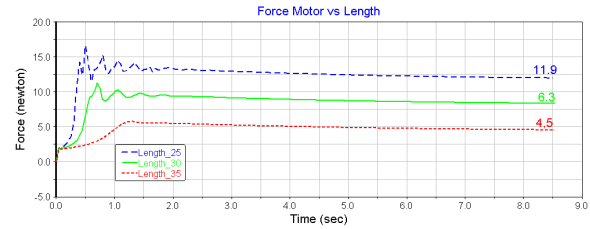

Fig. 6.   Simulation of the required force a motor should deliver when bars elongate up to 20cm.

nut to the extreme of the internal tube. Figure 7 shows this principle while (5) states the relation between W, the force generated by the mechanism, and M, the torque of the motor.

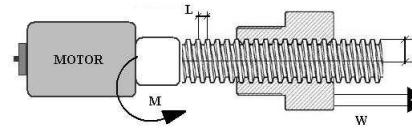$$M = W \tan\left(\arctan\left(\frac{L}{2\pi r}\right) + r \arctan(\mu)\right) \qquad (5)$$

Fig. 7.   Movement transmission between motor and screw.

Each bar has two aluminium tubes, one $(13x10.5mm)$ fitted within the other $(18x15mm)$ allowing its length vary from 55 to $95cm$. The motion system is composed by a DC motor (Faulhaber Series 2342), a metal gear head unit $(14 : 1)$ and a digital encoder $(16pulses/rev)$. The motor is located in the base of the bar (blue in figure 9) so that its shaft rotation makes the bar length to change. For integrity reasons each bar has been provided with two stop switches. When all the bars are built and ready mounting the full robot is as easy as joining the springs correctly and fix the lower nodes on the support table. Figure 8 shows the full robot architecture.

Looking at figure 8 we can see the robot has two kind of joints. The lower ones are spherical joints providing free movement of the bar in any direction of rotation. Please note that the springs should end at the same point where the joint is, this is what the mathematical model considers; instead they don't because of difficulties in the physical implementation.

Fig. 8.   Tensegrity based prototype robot.

The upper nodes just concentrate three springs each. Again, the node is not punctual so we may observe little differences between the real behaviour and the predicted one with the theoretical model. Finally, figure 9 includes a comparison drawing between the CAD designed bar and the real one, and details of the upper and lower nodes.
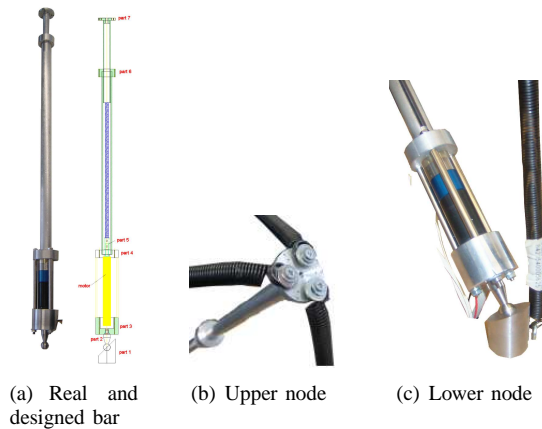

(a) Real and designed bar   (b) Upper node   (c) Lower node

Fig. 9.   Some details about the prototype structure.

C. Control hardware

The control hardware has been divided into two different parts: motion control and force acquisition unit. The first one deals with the movement of the each bar, sending and receiving commands, synchronizing movements, home method and so on. The second part is in charge of acquiring and sending the current force value of the six springs.

Let begin with the motion control unit. The Faulhaber MCDC2805 driver has been chosen for this application; it provides a standard RS-232 serial link with a bit rate up to $19.200baud$. As the used host computer had only one input serial port and we have three motors, we had to deal with:

1) Collisions. Every driver asynchronously sends a reply data package informing of the end of movement. As it is possible that two drivers send this at the same time a collision may occur. So transitions are placed in a multiple access.
2) Bandwidth. The maximum bandwidth available for a standard serial port is $115.200bps$. This means in our

particular case that every driver can use up to $38.400bps$. However, this baud rate may not be enough in the future if more information is required, like torque, sense current, etc., or more actuators are added to the structure.

Both problems were solved by implementing a switch serial port-Ethernet using a FPGA device providing a bandwidth up to $100Mbps$. Every device entering the switch has its own address so multiple access situations are avoided. Finally, an interface board between the FPGA and the computer is necessary to translate TTL levels to RS232 and vice-versa. Figure 10 depicts the schema of the motion control unit.
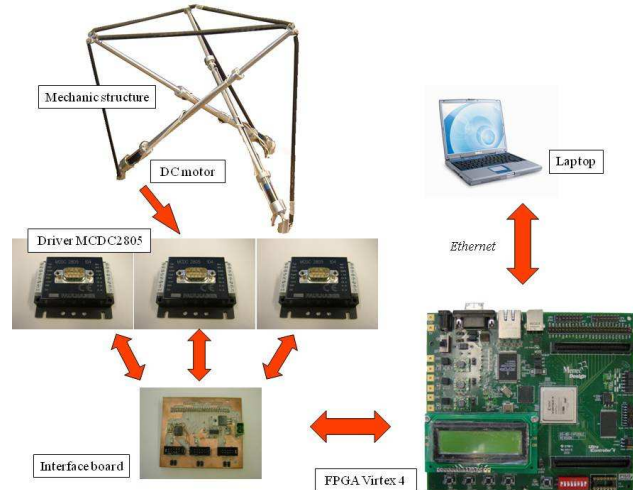

Fig. 10.   Motion control hardware diagram.

We now proceed with the force sensor acquisition unit. A measure of force in each spring provides a lot of insight to understand how the full structure acts and responds. As shown in figure 11, the force measure system comprises the load cells (Futek, LSB200), the signal conditioning (Texas Instruments SCC-SG24), the analog to digital converter (Analog Devices AD7939CB) and another FPGA (Xilinx Virtex4 ML405) which properly filters, calculates, and sends the force values to the host computer through an Ethernet port.
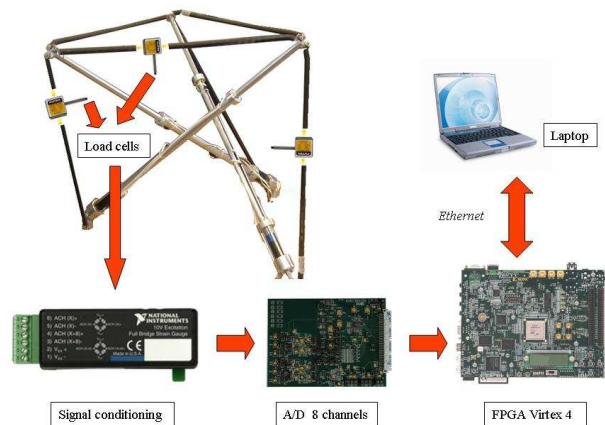

Fig. 11.   Force acquisition hardware diagram.

V. RESULTS

We present in this section two experiments performed with the real tensegrity based mechanism. The aim is to demonstrate the possibility of taking a tensegrity structure from an initial stable configuration to a desired one. This is equivalent to state that by means of changing the shape of the structure we can bring a specified point of the structure, the end effector, to a desired position in the space.

The first experiment shows how the structure changes height by moving the three actuated bars at the same velocity. Initial length for all the three bars is $670mm$, the final length is $920mm$ and the velocities are $1mm/s$. This corresponds to an almost pure vertical trajectory of the structure from $44cm$ to $70cm$ height. Figure 12 shows the forces gathered by the sensors: load cells 1 to 3 correspond to vertical springs while load cells 4 to 6 to the springs on the upper platform. Figure 13 contains two snapshots for the initial and final configurations of the structure.
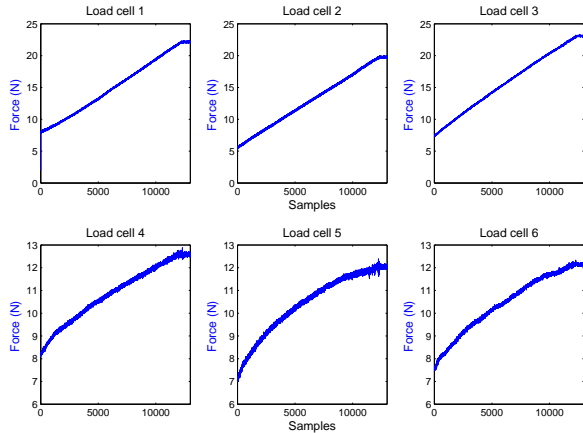

Fig. 12. Springs' real force when the three bars change length at equal rates.

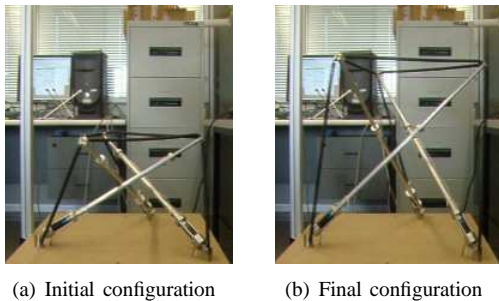(a) Initial configuration   (b) Final configuration

Fig. 13. Two snapshots from the vertical trajectory of the structure.

The second experiment shows a little bit more complex trajectory performed by the structure. Initial and final lengths for the actuated bars are the same as in the previous experiment, but now different velocities are given to each bar: 2, 4 and $8mm/s$. While the final configuration is exactly the same the performed trajectory is now a kind of three-direction steps ladder; the upper platform tends to move towards the bar with highest velocity. Again, the structure changes height between

44 and $70cm$ but this time simultaneously moving on the xy plane of the top platform. Figure 14 shows the forces gathered by the load cells. Some snapshots of the performed trajectory are shown in figure 15 where Matlab plottings have been used to give an upper view of the structure (projected onto the $x-y$ plane) and hence a clearer understanding of the performed trajectory.
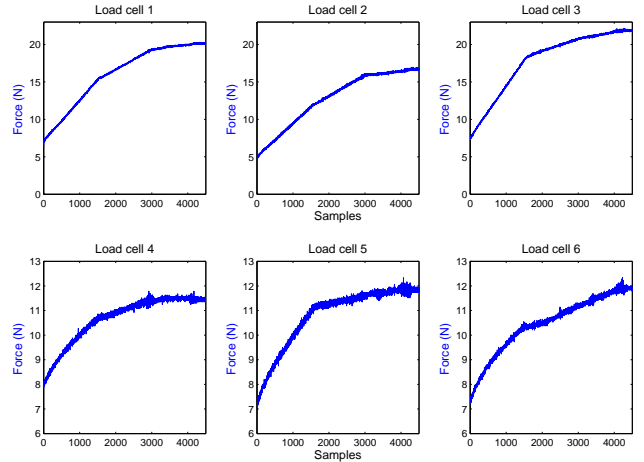

Fig. 14. Real force on the springs when the three bars change length at different velocities.

(a) t=5s   (b) t=10s

(c) t=15s   (d) t=20s
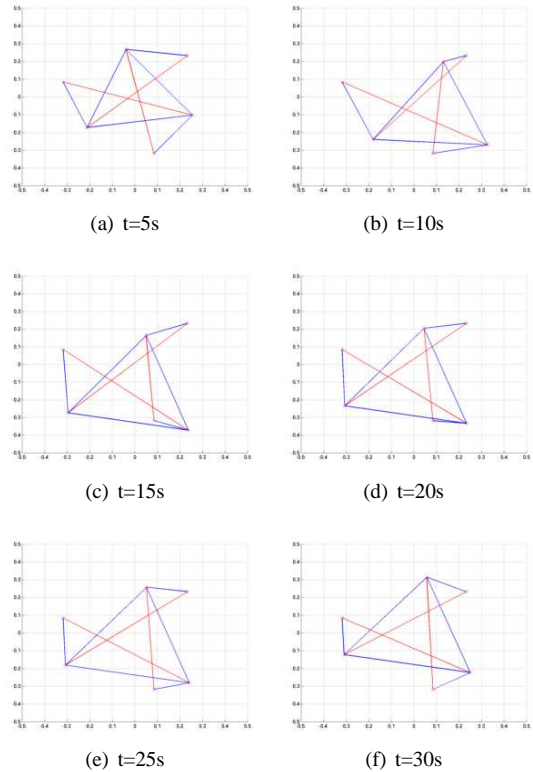
(e) t=25s   (f) t=30s

Fig. 15. Some snapshots for a trajectory considering different bar velocities. In this experiment $v_{b_1} = 2$, $v_{b_2} = 4$ and $v_{b_3} = 8mm/s$.

VI. CONCLUSIONS

Obtaining new kind of deformable robots using tensegrity structures having some or all of its elements actuated is nowadays a big challenge for roboticians. In the case that more elements than degrees of freedom in the space are actuated we obtain a hyper -actuated device which may be, apart of moved, shape controlled. The objective of this paper has been to demonstrate the application of these structures to develop robotic mechanisms.

This paper has been devoted to explain how our first prototype of tensegrity based robot was developed. Based on a 3-bar tensegrity prism, we allow its bars to change length which gives us the possibility to control three degrees of freedom in the space. Those are the height of the structure as well as the xy position of the upper platform. The workspace of the mechanism was presented in figure 2 demonstrating the feasibility of performing a shape-changing structure that can perform any trajectory inside this workspace. We note, however, the taken decision to use springs as passive elements which accommodate themselves to the resulting structure for each stable configuration. This translates into an under-actuated device, that is it has more degrees of freedom than the ones we can effectively control. In despite of this we still were able to perform arbitrary trajectories within the workspace assuming no external forces other than gravity were acting on the structure.

We notice here the singularity of the equilibrium matrix for a stable tensegrity configuration. This means that although cables can be used that rigidifies the structure so avoiding unwanted motions when applying external forces to the nodes, an infinitesimal mechanism exists which, in this case, would allow infinitesimal rotations of the upper platform with respect the base. This effect can be negligible using enough pre-tensioned cables. Also, a non-minimal tensegrity configuration would not have this infinitesimal mechanism, for instance the one with a completed topology graph, with extra cables between nodes (n_2, n_6), (n_3, n_4) and (n_1, n_5). For the purpose of demonstrating that some or all of the elements of a tensegrity can be actuated to obtain a deformable structure that, in medium term, can be used as a deformable mobile robot, we have found the minimal tensegrity configuration interesting by itself.

We did neither focused the paper on how to obtain a proper control law for the designed robot, instead we presented an open-loop law based in the form-finding process used. Author's are currently working on a control law that, given a goal point, provides the necessary length changes of the structure's elements so as to achieve the goal in a required time. Results already exist in the literature for tensegrity driven by tendon, see for instance the work by [12], although nobody dealt before with bar actuation. Kinematics and dynamics of tensegrity structures are difficult to solve because of the involved equations. In fact, the issue of how to control the structure to change its shape as well as to move it remains an open and challenging question in the literature. We also shall investigate in the near future how to combine actuated bars and cables so as to have a hyper-actuated structure.

Despite their huge potential of applicability only a few structures of this kind have been built at the present time. Tensegrity have already been shown to have superior features than traditional approaches in areas like architecture or civil engineering, and some of their properties, such as high energetic efficiency, deploy-ability, deform-ability and redundancy, as well as their biological inspiration, make this kind of structures good candidates to design both mobile robots and manipulators. So we think that a good field of application for such structures is to allow them move by the use of adequate actuators and sensors, and expect that in the next years research on tensegrity structures will focus on their dynamics and control, and, in our specific interest, obtaining new deformable and totally environmental adaptable robots. We just gave an example in this paper of a novel functional tensegrity robot based on a compliant passive tendon network actuated by a bar-length controller hardware.

REFERENCES

[1] J.B. Aldrich. *Control synthesis for a class of light and agile robotic tensegrity structures*. PhD thesis, University of California, 2004.

[2] R. Connelly. Rigidity and energy. *Inventiones Mathematicae*, 66:11–33, 1982.

[3] R. B. Fuller. *Synergetics, explorations in the geometry of thinking*. Collier Macmillan, 1975.

[4] A. Graells-Rovira and J.M. Mirats-Tur. Control and simulation of a tensegrity-based mobile robot. *Robotics and Autonomous Systems*, 57(5):526–535, 2009.

[5] S. Hernández and J.M. Mirats-Tur. Tensegrity frameworks: Static analysis review. *Int. Journal of Mechanism and Machine Theory, available on line August 2007*, 2007.

[6] S. Hernández and J.M. Mirats-Tur. A method to generate stable, collision free configurations for tensegrity based robots. *IEEE/RSJ 2008 International Conference on Intelligent Robots and Systems, IROS08, 22-26 Sep., Nice, France*, 2008.

[7] D.E. Ingber. Cellular tensegrity: defining new rules for biological design that govern the cytoskeleton. *Journal of Cell Science*, 104:613–627, 1993.

[8] D.E. Ingber. Architecture of Life. *Scientific American*, 52:48–57, 1998.

[9] M. Kanchanasaratool and D. Williamson. Motion control of a tensegrity platform. *Communications in Information and systems*, 2(3):299–324, 2002.

[10] H. Kebiche, M.N. Kazi-Aoual, and R. Motro. Geometrical non-linear analysis of tensegrity systems. *Journal of Engineering structures*, 21:864–876, 1998.

[11] S.M. Levin. The tensegrity-truss as a model for spinal mechanics: Biotensegrity. *Journal of mechanics in medicine and biology*, 2(3), 2002.

[12] M. Masic and R.E. Skelton. Path planning and Open-Loop Shape Control of Modular Tensegrity Structures. *AIAA Journal of Guidance, Control and Dynamics*, 28 (3):421–430, 2003.

[13] M. Masic and R.E. Skelton. Open-loop control of class-2 tensegrity towers. *Proceedings of SPIE*, 5383:298–308, 2004.

[14] J.M. Mirats, S. Hernandez, and A. Graells. Dynamic equations of motion for a 3-bar tensegrity based mobile robot. In *Proceedings of the 12th IEEE Conference on Emerging Technologies and Factory Automation, Patras, Greece*, 2007.

[15] R. Motro, S. Najari, and P. Jouanna. Static and dynamic analysis of tensegrity systems. In *Proceedings of the ASCE International Symposium on Shell and Spatial Structures: Computational aspects*, pages 270–279. Springer, 1986.

[16] H. Murakami. Static and dynamic analysis of tensegrity structures. Part 1: Nonlinear equations of motion. *International Journal Solids and Structures*, 38:3599–3613, 2001.

[17] C. Paul, F.J. Valero-Cuevas, and H. Lipson. Design and Control of Tensegrity Robots for Locomotion. *IEEE Transactions on Robotics*, 22(5):944–957.

[18] S. Pellegrino. Analysis of prestressed mechanisms. *International Journal Solids and Structures*, 26(12):1329–1350, 1989.

[19] R.E. Skelton, J.P. Pinaud, and D.L. Mingori. Dynamics of the shell class of tensegrity structures. *Journal of Franklin Institute*, 338:255–320, 2001.

[20] K.D. Snelson. Continuous tension, discontinuous compression structures. United States Patent 3169611, February 1965.

[21] C. Sultan. *Modeling, design and control of tensegrity structures with applications*. PhD thesis, Purdue Univeristy, 1999.

[22] C. Sultan, M. Corless, and R.E. Skelton. Linear dynamics of tensegrity structures. *Journal of Engineering structures*, 24:671–685, 2002.

[23] A.G. Tibert and S. Pellegrino. Review of form-finding methods for tensegrity structures. *International Journal Solids and Structures*, 18(4):209–223, 2003.

[24] S.P. Timoshenko and D.H. Young. *Cats' Paws and Catapults: Mechanical Worlds of Nature and People*. W. W. Norton and Company, 2000.